Dependence of spatial coherence of coherent suppression of magnetization precession upon aspect ratio in Ni81Fe19 microdots

A. Barman, V. V. Kruglyak, R. J. Hicken, J. Scott, and M. Rahman

Additional information on J. Appl. Phys.

Dependence of spatial coherence of coherent suppression of magnetization precession upon aspect ratio in Ni$_{81}$Fe$_{19}$ microdots

A. Barman, V. V. Kruglyak, and R. J. Hicken[a)]
School of Physics, University of Exeter, Stocker Road, Exeter EX4 4QL, United Kingdom

J. Scott and M. Rahman
Department of Physics and Astronomy, University of Glasgow, Glasgow G12 8QQ, United Kingdom

(Presented on 10 November 2004; published online 28 April 2005)

Coherent suppression of magnetization dynamics in circular microdots of Ni$_{81}$Fe$_{19}$ has been observed by time-resolved scanning Kerr effect microscopy. The applied pulsed field rose sharply, stimulating precession, and then exhibited an oscillatory behavior. For certain values of the static magnetic field the precession was suppressed at the point at which the magnetization lay in the sample plane. Time resolved images confirmed that coherent suppression had occurred at the center of the element, but nonuniformity was observed at the edges of the element, which became greater with decreasing aspect ratio. The nonuniform magnetization dynamics result from the dephasing of confined spin wave modes, suggesting that a more involved pulse shaping scheme may be required to coherently suppress the full mode spectrum. © *2005 American Institute of Physics.* [DOI: 10.1063/1.1850834]

Recent developments in magnetic data storage technology require ultrafast magnetic switching to be achieved and understood in micro- and nano-magnets. While precessional switching may be sufficiently fast, "ringing" imposes a lower limit on the time delay between consecutive switching processes, and must be controlled by careful optimization of the damping parameter. Alternatively, attempts have been made to control precession by tailoring the applied magnetic field pulse.[1,2] Gerrits *et al.*[1] demonstrated precessional switching in an elliptical element by suppressing the precession after half a cycle, while coherent suppression of magnetization dynamics has been observed in magnetic single layer and multilayer structures.[3–5] However, the spatial uniformity of precessional switching remains a subject of continuing debate,[2,6] and the spatial character of coherent suppression has not yet been studied in magnetic elements with lateral dimensions of just a few microns. Nonuniform eigenmodes have been observed in confined magnetic structures, their character depending on the shape and aspect ratio of the structure.[7–11] It is therefore interesting to study the spatial coherence of coherent suppression of precession in such structures. Here, we have employed time-resolved scanning Kerr effect microscopy to study the spatial coherence of coherent suppression in circular microdots of Ni$_{81}$Fe$_{19}$. Micromagnetic simulations have also been used to understand the experimental results.

A series of circular Ni$_{81}$Fe$_{19}$ elements of varying aspect ratio was studied. We label the samples as S1 (width $=10$ μm, thickness$=22$ nm, aspect ratio$=$width/thickness $=454$), S2 (width$=7$ μm, thickness$=22$ nm, aspect ratio $=318$), S3 (width$=5$ μm, thickness$=22$ nm, aspect ratio $=227$), and S4 (width$=10$ μm, thickness$=150$ nm, aspect ratio$=67$). The Ni$_{81}$Fe$_{19}$ was deposited either by evaporation (S1–S3) at a base pressure of 2×10^{-6} Torr, or by sputtering

(S4) from a base pressure of 2×10^{-7} Torr, onto a bilayer of patterned poly(methylmethacrylate) resist which was then lifted off to leave the sample elements. Magneto-optical pump-probe measurements were performed with a time-resolved scanning Kerr effect microscope[12] using a Ti–sapphire laser with 120 fs pulse width, 80 MHz repetition rate, and 800 nm wavelength. An in-plane pulsed field **h** was generated by a pulsed current triggered by a photoconductive switch and delivered to the samples either by a co-planar waveguide (S1–S3) in which the central conductor was 12 μm wide, or a co-planar stripline (S4) structure with track width and separation equal to 30 μm. Both structures were formed by deposition of Au onto GaAs. The pulsed field profile was characterized by electro-optic sampling in a 0.5-mm-thick LiNbO$_3$ crystal placed on the transmission line.[12] The probe was focused to a submicron spot using a microscope objective (numerical aperture$=0.65$) and the sample was scanned under the probe spot to acquire time-resolved images. The instantaneous out-of-plane magnetization component was probed by the polar magneto-optical Kerr effect. A static field **H**, of strength H was applied within the plane of the sample.

The experimental geometry is shown in Fig. 1(a). Figure 1(b) shows that for S1–S3 the pulsed field rises within about 40 ps. Impedance mismatches between the photoconductive switch, transmission line and power supply were sufficiently large as to produce an oscillatory magnetic field, with period of about 400 ps, that we exploit in the present study. The peak field amplitude was estimated to be 30–40 Oe. Figure 1(c) shows the time dependent Kerr rotation obtained from S1, at three different values of H, when the probe beam was focused at the center of the element. For $H=145$ and 732 Oe, long-lived precessional motion occurs for the full experimental time scale (1.8 ns), while for $H=400$ Oe, the precessional motion stops abruptly after one full cycle of precession. The precession may be described by the Landau–Lifshitz–Gilbert equation. For precession to be suppressed, the magnetization

[a)]Author to whom correspondence should be addressed; electronic mail: r.j.hicken@ex.ac.uk
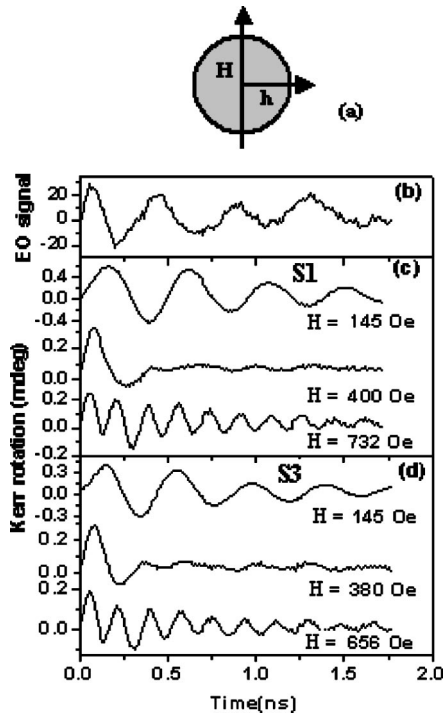
FIG. 1. (a). The experimental geometry is shown. The (b) pulsed field profile, and the measured time dependent Kerr rotations are shown for samples (c) S1 and (d) S3. The values of the static field H are shown within the figure.
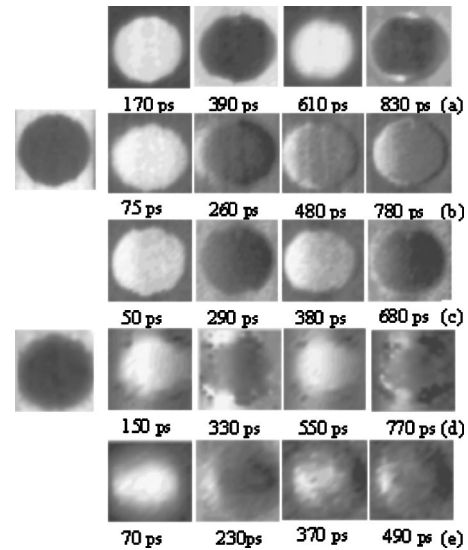

FIG. 2. The time-resolved Kerr images obtained in the geometry of Fig. 1(a) are shown for (a) S1, $H=145$ Oe; (b) S1, $H=400$ Oe; (c) S1, $H=732$ Oe; (d) S3, $H=145$ Oe; and (e) S3, $H=380$ Oe. The delay times are shown under each image. Intensity images are presented in the column on the left for comparison.

M must first become aligned with the total effective field so that the torque upon the magnetization vanishes, and thereafter the total effective field must only change slowly. Since **H** and **h** lie within the sample plane (we neglect the small in-plane uniaxial anisotropy) and the demagnetizing field is antiparallel to the out-of-plane magnetization component, the magnetization can only become parallel to the total effective field if the magnetization lies within the sample plane. Suppression may then only be achieved for certain values of **H** such that **H**+**h** is parallel to **M** at this instant in time. From Fig. 1(c) we see that suppression indeed occurs at the point at which the out-of-plane component of magnetization vanishes.

In order to study the spatial character of the suppression mechanism, time-resolved images of S1 were acquired for the values of H used in Fig. 1(c), and are presented in Figs. 2(a)–2(c) for four different time delays. The physical area of the element is shown by the intensity image included at the left. The gray scale represents the out-of-plane component of the instantaneous magnetization. At $H=145$ and 732 Oe, alternative white and black contrast is observed in images obtained at positive and negative antinodes of the precessional motion, respectively. The images at all time delays are spatially uniform apart from very small nonuniform edge regions perpendicular to the direction of **H**. For $H=400$ Oe, where coherent suppression is expected to occur, the time resolved images are white and black at the first positive and negative antinodes before becoming gray after precession has been suppressed.

Figure 1(d) shows the time dependent Kerr rotation observed at the center of S3 for $H=145$ Oe, $H=380$ Oe and $H=656$ Oe. For $H=145$ and 656 Oe, long-lived precession is

seen, whereas for $H=380$ Oe, coherent suppression is achieved. The spatial character of the coherent suppression was again studied through the acquisition of time-resolved images at $H=145$ and 380 Oe. The images are shown in Figs. 2(d) and 2(e) with their width scaled to match those in (a)–(c). The variation in contrast from left to right in the S3 images is an artifact resulting from a slight misalignment of the sample, whereas the variation in contrast from top to bottom shows the homogeneity of the magnetic response. At $H=145$ Oe the central region alternates between light and dark at positive and negative antinodes, but the nonuniform edge regions perpendicular to **H** are found to be proportionately larger than for S1. Consequently, for $H=380$ Oe the first two antinodes show light and dark contrast, and after coherent suppression has occurred, the images become gray, but with greater nonuniformity at the upper and lower edges than observed for S1. The nonuniform magnetic response cannot result from spatial nonuniformity of the pulsed field, or else the response of S1 would be expected to be less rather than more uniform than that of S3.

In a finite nonellipsoidal magnetic element, free magnetic poles at the edges of the element generate a nonuniform demagnetizing field in the static configuration. Regions where the demagnetizing field is nonuniform provide dynamic pinning and confined spin waves have been observed after application of a pulsed field both within the central region of the element[8,9] and at the edges.[7,10] The confinement depends upon the shape and aspect ratio of the elements. In order to study the effect of aspect ratio on the generation of spin waves in circular microdots we acquired time-resolved images of S1–S4. The time dependent Kerr rotation measured at the center of each element is shown in Fig. 3, with the scan for S4 clearly showing beating. The fast Fourier transform (FFT) spectra of S1–S3 show a single resonance mode but S4 shows two resonant modes. The time-resolved images of S1–S4 are presented in Fig. 4 for four different
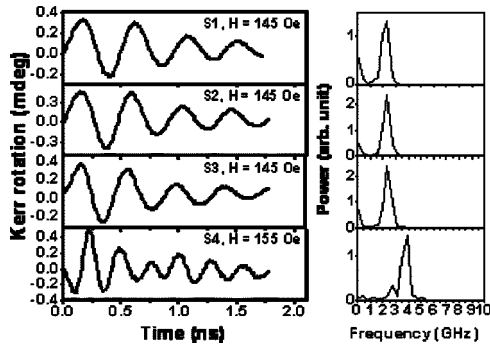
FIG. 3. The measured time dependent Kerr rotations are shown for (a) S1, $H = 145$ Oe, (b) S2, $H = 145$ Oe, (c) S3, $H = 145$ Oe, and (d) S4, $H = 155$ Oe. The right hand panels show the corresponding FFT power spectra, while the experimental geometry is similar to Fig. 1(a).

FIG. 4. (a) The time-resolved Kerr images obtained in the geometry of Fig. 1(a) are shown for S1, $H = 145$ Oe; S2, $H = 145$ Oe; S3, $H = 145$ Oe; and S4, $H = 155$ Oe. The delay times are shown under each image while intensity images are shown in the column at the left for S1–S3. (b) The simulated magnetic images before application of the pulsed field **h** are shown.

time delays. The variation in contrast from left to right within the images of S2 and S3 is an artifact as mentioned previously. Nonuniformity is confined to near the edges perpendicular to **H**, becoming proportionally larger from S1 to S3. However, for S4, the nonuniformity also spreads into the central area of the element, with a stripe pattern developing due to dephasing of spin wave modes within the central region.

Micromagnetic simulations, performed with the OOMMF software,[13] of the magnetization before the application of the pulsed field are shown in Fig. 4(b). The samples were divided into 250×250 cells and the arrows in each simulated image represent the in-plane magnetization sampled over 20 cells. The simulated images clearly show that the edge regions become more nonuniform from S1 to S4, as the aspect ratio decreases. These regions pin the spin waves excited in the center of the element and may confine additional modes at the edges. Coherent suppression requires the phase of the precession to be matched to that of the pulsed field in the manner described previously. The phase of the precession depends upon the mode frequency, which can be controlled by adjusting H, as was shown for S1. However, when multiple modes of different frequency are present, the condition for suppression cannot be achieved for all modes simultaneously. In the case of S3, precession may therefore continue at the edges after suppression has been achieved at the center.

In conclusion, we have observed coherent suppression of magnetization precession in circular microdots of $Ni_{81}Fe_{19}$. The pulsed field rose within about 40 ps before oscillating with a period of about 400 ps. Coherent suppression was achieved by adjusting the static field so that there was no net torque acting upon the magnetization after one cycle of precession. The coherent suppression became more spatially nonuniform as the aspect ratio of the element was decreased. Time-resolved Kerr images and simulations of the demagnetizing field within samples with aspect ratio in the range of 454–67 suggest that increased nonuniformity results from confinement and dephasing of multiple spin wave modes. For samples of smaller aspect ratio and/or lower symmetry, where the splitting of the mode frequencies increases, a simple pulse-tailoring scheme will be less effective in sup-
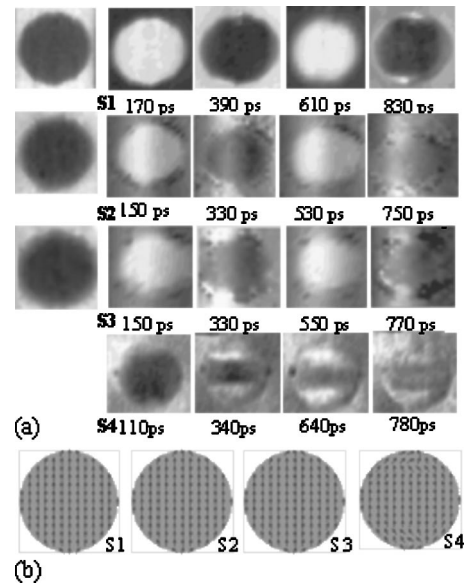
pressing precession and may lead to increased high frequency magnetic noise. A more involved pulse-shaping scheme[14] may be required to suppress all resonant modes so that spatially uniform precessional switching may be achieved in confined magnetic structures of arbitrary shape and aspect ratio.

[1]T. Gerrits, H. A. M. van den Berg, J. Hohlfeld, L. Bar, and T. Rasing, Nature (London) **418**, 509 (2002).

[2]W. K. Hiebert, L. Lagae, and J. De Boeck, Phys. Rev. B **68**, 020402 (2003).

[3]T. M. Crawford, P. Kabos, and T. J. Silva, Appl. Phys. Lett. **76**, 2113 (2000).

[4]M. Bauer, R. Lopusnik, J. Fassbender, and B. Hillebrands, Appl. Phys. Lett. **76**, 2758 (2000); M. Bauer, R. Lopusnik, H. Dotsch, B. A. Kalinikos, C. E. Patton, J. Fassbender, and B. Hillebrands, J. Magn. Magn. Mater. **266–230**, 507 (2001).

[5]H. W. Schumacher, C. Chappert, P. Crozat, R. C. Sousa, P. P. Freitas, and M. Bauer, Appl. Phys. Lett. **80**, 3781 (2002).

[6]T. J. Silva, P. Kabos, and M. R. Pufall, Appl. Phys. Lett. **81**, 2205 (2002).

[7]J. P. Park, P. Eames, D. M. Engebretson, J. Berezovsky, and P. A. Crowell, Phys. Rev. Lett. **89**, 277201 (2002).

[8]A. Barman, V. V. Kruglyak, R. J. Hicken, J. M. Rowe, A. Kundrotaite, J. Scott, and M. Rahman, Phys. Rev. B **69**, 174426 (2004).

[9]A. Barman, V. V. Kruglyak, R. J. Hicken, J. Scott, A. Kundrotaite, and M. Rahman, J. Appl. Phys. **95**, 6998 (2004).

[10]J. Jorzick, S. O. Demokritov, B. Hillebrands, M. Bailleul, C. Fermon, K. Y. Guslienko, A. N. Slavin, D. V. Berkov, and N. L. Gorn, Phys. Rev. Lett. **88**, 047204 (2002).

[11]M. Belov, Z. Liu, R. D. Sydora, and M. R. Freeman, Phys. Rev. B **69**, 094414 (2004).

[12]A. Barman, V. V. Kruglyak, R. J. Hicken, A. Kundrotaite, and M. Rahman, IEE Proc.: Sci., Meas. Technol. **150**, 260 (2003).

[13]M. Donahue and D. G. Porter, OOMMF User's guide, Version 1.0, Interagency Report NISTIR 6376, NIST, Gaithersburg, MD, 1999: URL: http://math.nist.gov/oommf

[14]T. Brixner and G. Gerber, ChemPhysChem **4**, 418 (2003); H. Rabitz, R. de Vivie-Riedle, M. Motzkus, and K. Kompa, Science **288**, 824 (2000).